A STUDY ON USING PRE-SURFACE GEOMETRY IN INERTIA FRICTION WELDING PROCESS

Khalil Ibrahim ABASS[1], Mohammed Abdulraoof ABDULRAZZAQ[2]

Inertia Friction Welding (IFW) is one of the most economical and efficient "solid-state joining" production methods for joining similar and dissimilar materials. Plastic deformation of interface material is the essence of friction welding. The principle of the process is that one of the parts to be jointed remains fixed, while the other is rotated at a high speed and then brought in contact, under pressure, with the fixed part. In this study, an IFW investigation was carried out on five series of pre-surface contact profiles. The comparison is considered for each of these series referring to traditional inertia friction welding type. Similar Aluminum 1100 material is used. Evaluation of metallographic cross-section and microhardness properties interface is showed and presented in all welds. The results obtained by the analysis of the IFW joints showed that the geometry of the contact surfaces influences the distribution of the flash material, the microhardness values in deformed areas and the length of axial upset of the welded assembly.

Keywords: Friction welding, Inertia friction welding, Rotary friction welding, Microhardness testing.

1. Introduction

The friction welding process is defined as any joint between two workpiece parts resulting under pressure and heat conditions that are generated by the friction state at the interface contact. In a modification of this process, called Inertia Friction Welding (IFW), the energy is supplied through a flywheel, which finally comes to a stop as the weld is formed [1]. The principle of the process is showed in Figure 1.

In stage I, the two parts are brought in contact, which results in an increase in the friction, a slowing in the rotation speed due to the dry friction between the interfaces (Fig. 1-stage I). In stage II, the friction resulted in thermo-mechanical deformation, making the interface completely plasticized (Fig. 1-stage II). In stage III, the forging force is being applied with drop in rotation speed, the torque grows to peak value for overcoming the hardening and cooling. The flash is formed due to refining the interface microstructure, which leads to additional cooling at the bond circumference (Fig. 1-stage III) [2].

[1] PhD, Mustansiriyah University, College of Engineering, Mechanical Engineering Department, Baghdad, Iraq, e-mail: khalil1969a@yahoo.com, k.i.abass@uomustansiriyah.edu.iq
[2] PhD, Mustansiriyah University, College of Engineering, Materials Engineering Department, Baghdad, Iraq, e-mail: mohammedraof415@yahoo.com, drmohammedraoof@uomustansiriyah.edu.iq

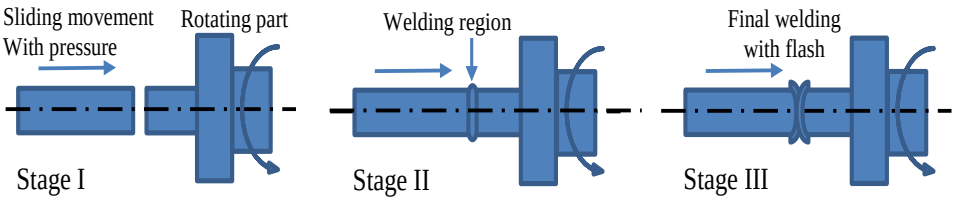

Fig. 1. Stages of the inertia friction welding, IFW

The proper control of energy and pressure makes the metal work thoroughly, the bond is clean and stronger than the base metal, and the results are uniform from piece to piece. The operation emits no bright light, sparks, fumes, or loud noises [3]. The advantages of the process are the use in joining metal and non-metals, similar and dissimilar parts, high quality, short time for producing, no adding materials such as flux or filler, less affected heat area in the process. The disadvantages of the IFW are the use for smaller parts of machines, very high cost of setup, critical preparation of the workpiece and limit for flat and angular joints. The applications of the IFW are used in various industries (electrical and mechanical): automobile, aerospace, oil, and marine [4].

2. Literature review

In order to establish the weld quality, the combined effects of the heat transfer and mechanics are concerned in the friction joint parts. The friction well-meant of similar parts material austenitic stainless steel (AISI 304) [5], pearlitic steel bars [6], and dissimilar parts material HSS steel M2-carbon steel 1060 is presented [7] and the mild steel-bronze have been investigated [8], dissimilar friction welded γ-TAB-Ti64 joints [9], while ductile cast iron-stainless steel interface was measured [10].

The weld quality and optimizing the friction welding parameters are studied. The processed joints were tested for their microstructure and strength related aspects. Additionally, for deciding near-optimal process parameters settings, a "Genetic Algorithm" method is proposed. The tensile tests showed that joint strength decreased with an increase in the friction time. The micro Vicker's hardness increases with increasing friction time. Trials under optimum welding conditions resulted in good joint strengths, which were in fair agreement with the predicted results [5].

Two orbital FE models by inertia friction welding of pearlitic steel bars have been modeled. The microstructure evolution of the thermo-metallurgical model and the temperature profile of the coupled thermo-mechanical model are analyzed. It is observed and predicted experimentally that due to the cooling rates, high heating and steep temperature gradient a high quantity of martensite is shaped, which is detrimental to the weld toughness. The predicted model can be used to achieve a

suitable pre-and/or post-weld heat treatment [6]. The characteristic zones of the friction-welded layer are established as illustrated in the physical model (surfaced layer, viscous layer, visco-plastic layer, friction plane, carbide plane, mixing zone, and other zones). The biggest differences in properties were determined within the area of the viscous layer and carbide plane [7].

The effect of the friction pressures and upset time on the microstructure, tensile and hardness properties of the mild steel and bronze welds were investigated. The welds showed better metallurgical and mechanical properties that result from the fusion welding techniques. The hardness values increase with any increase in friction and upset pressure. The tensile strength of the obtained weld joints can reach base metal strength of 70% if suitable welding parameters are determined. Re-crystallized well and elongated grains were obvious together on the welded surface [8].

Dissimilar friction welded of γ-TAB-Ti64 joints (the intermetallic γ-TiAl based alloy Ti-47Al-3.5(Mn+Cr+Nb)-0.8(B+Si) (denoted as γ-TAB) is used for describing microtexture and microstructure development. The diffusion process was controlled by very short process duration. It was found that the intermetallic is more sensitive to the applied friction welding parameters used in this research. Microstructure transformation as well as grain refinement led to local development of the friction welded joints [9]. Tensile strength and hardness tests of the ductile cast iron-stainless steel joints were using to determine the quality of the intersections in the friction welding parts. Additionally, light metallography and electron microscopy were used for the microstructure examination. The research has documented that the high temperature of the IFW process leads to grain structure formation and changing dislocation continuously [10].

The finite element method (FEM), numerical simulation and experiments have been prepared to analyse the FW process, which is a process with a transient operation, high temperature, and large deformation. The combined effects of the heat transfer and mechanics are taken into account in the joint part. The mechanical deformation, temperature fields, strain, strain rate, and stress were numerically evaluated [11].

The combined effects of the heat transfer and mechanics of friction welding in the mathematical model are presented. The simulation results, von Mises stress, strain, deformation, and temperature distributions were mathematically evaluated. The investigation concluded that the prediction model can be used as an evolution tool of the welded parts final geometry [12].

This research focuses on using five series of contact surface profiles "Aluminum 1100" in inertia friction welding and evaluating the product profile, hardness distribution after usage. The analysis uses a simple way to calculate the four levels of hardness, inside and outside of the product. Additionally, it compares the levels of hardness average values of each profile in order to establish the best profile surface area resulting in the best quality of the product.

3. Experimental work

3.1. Primary surface contact, expression and classification

The first step of the analysis is selecting thirteen surface profiles of the inertia friction welding specimen "Aluminium 1100". The profiles design in detail is shown in Figure 2. The selection depending upon the contact surface profile is classified into five series: Serie 1: B C D, Serie 2: E F G, Serie 3: H I, Serie 4: J K and Serie 5: L M. The comparison is considered for each of these series referring to traditional inertia friction welding type, A. The specimen involves two parts, effective and holder part (diameter x length), 15 x 30 mm and 12.5 x 20 mm respectively.

The study involves three main classifications, as illustrated in Fig. 2 and 3.
I) Fixed surface contact, traditional inertia friction welding type, A.
II) Single surface contact, with different surface profiles: point-extends to curve, B, C, and D; point-extends to plane surface, E, F and G; surface-extends with the fixed area, H, and I; and surface-extends with the incremental area, J and K.
III) Multi-surface contact, with different surface profiles, L and M.

Traditional Case A: Higher contact area "high pressure is requiring", the moment requirements for maintaining the rotatory state is high. Annealing time for essential welding temperature is high, due to the high amount of metal required for heating.

All these conditions require high primary energy for ensuring and maintaining start contact process resulting in a strong and resistant welding region necessary for subsequent machining conditions. The boundary conditions of the surface contact series 1-5 are represented in Fig. 4 and 5, during axial movement.

Serie 1, Cases B, C, D: comparing to traditional Case A: primary contact area increases by the pressure; obtaining annealing time gradually; the metal amount required for heating is lower, therefore, the moment requirements for maintaining the rotatory state are low.

Serie 2, Cases E, F, G: the same behaviour as that of Serie 1 "by low graduation", following the curvature behaviour of the surface contact area.

Serie 3, Cases H, I: Two stages of the surface contact area, 5 mm to 15 mm diameter and 10 mm to 15 mm diameter, maintain rising the temperature by two stages.

Serie 4, Cases J, K: Two stages of the surface contact area with 45° slid angle for both cases, 5 mm to 15 mm diameter and 10 mm to 15 mm diameter, maintain rising the temperature by two stages.

Serie 5, Cases L, M: Case L; maintain the contact area by three circular regions at the same time, 13, 10 and 5 mm, up, middle and down diameter respectively. Case M; maintain the contact area by the small selective areas distributed on the surface.

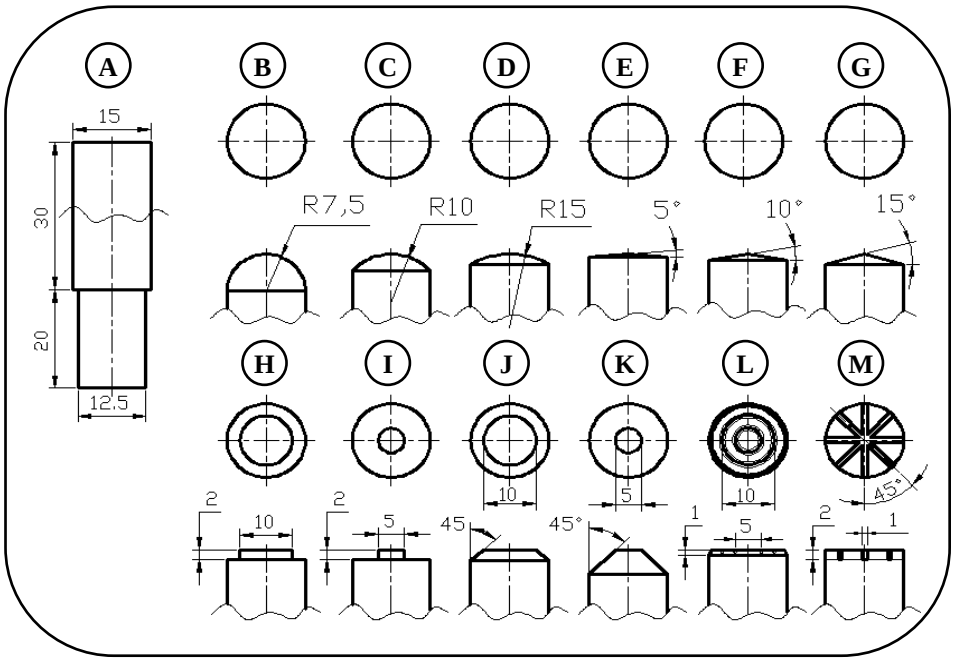

Fig. 2. Welding specimen surfaces plan

Fig. 3. Types of pre-surface used in inertia friction welding process

3.2. Boundary conditions

The chemical composition of the specimen material is presented in Table 1. Similar Aluminium 1100 specimens were joined by the inertia friction welding process. The parameters used for this study are presented in Table 2.

The work focuses on continuously driven inertia friction welding. The rotating motion of the component to be welded has a constant spindle rotation speed, n = 2000 rpm and the other component to be welded is pushed toward the rotating part by sliding. Alloy Aluminium 1100 round bar samples are welded by continuous drive inertia friction welding. The welding process limitations are the following: axial friction pressure, P_f = 95 MPa; friction time, t_f = 5 s; upsetting pressure, P_u = 150 MPa; and upsetting pressure time, t_u = 8 s.

Table 1

Chemical composition of 1100 Aluminum, wt. %

Al	Mn	Fe	Ni	Cu	Zn
99.07	0.19	0.43	0.00	0.31	0.00

Table 2

IFW parameters range values

Input variable	Friction pressure, P_f	Friction time, t_f	Upsetting pressure, P_u	Upsetting time, t_u
Range	80-100 MPa	3-8 s	140-160 MPa	5-10 s

Isometric 3D-design of the IFW principle is represented in the Fig. 4. The boundary conditions of the part surface contact area during axial movement are represented in the Fig. 5. The range of the penetrations of the welded parts is extended to 4 mm for the rotary side.

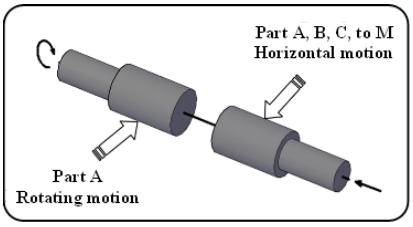

Fig. 4. 3D - isometric of the IFW principle

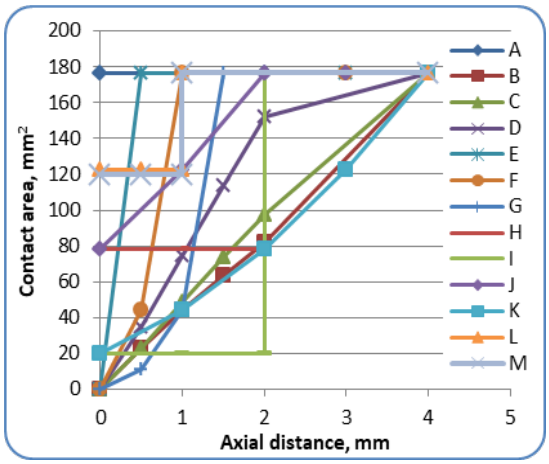

Fig. 5. Contact boundary conditions during axial movement

Practical steps of inertia friction welding process are presented in Fig. 6, by i) preparing the specimens, ii) welding process procedure, iii) removing the flash, and iv) preparing the welded parts for microstructure and microhardness tests. Additionally, Fig. 7 shows the photograph of all the jointed specimens and the preparations for tests.

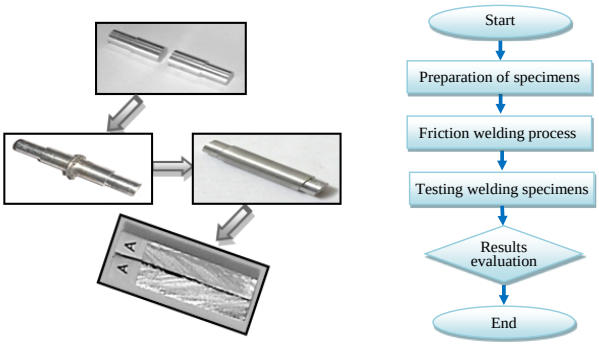

Fig. 6. Procedures of the friction welding process

Fig. 7. A photograph of specimens after IFW process, initially and after the flash was removed

3.3. Select the proper test

The joining applications (oil piping welding, plate welding, etc.) do not necessarily need high surface finishing procedures "outside surface". Therefore, the evaluations of the welded parts are involving the entire welding region "with the flash or the additional material". The sliding applications need smooth and hard surfaces for maintaining the contact movement without the wearing effect of both surfaces. The primary stage of this work considered the resulted parts used in the frictional applications (rotary or sliding shaft) with high surface finish quality. The microstructure of the inertia friction welded similar Aluminium 1100 joints was categorized into three different regions. The recrystallization zone adjacent to the bonding interface, the un-recrystallization zone "where the grains deformed and grown partly" and the un-deformed zone base material microstructure region, Fig. 8.

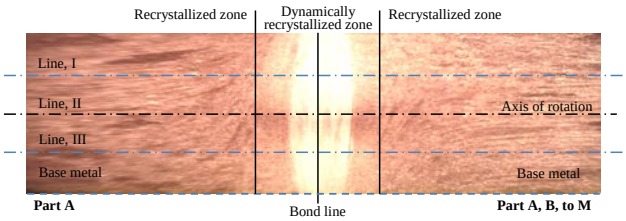

Fig. 8. Schematic picture of the grain structure in inertia friction welds

4. Discussion

4.1. Microstructure preview: The microscopic photographs presented in Fig. 9. The principle of the quality evaluation depends on three factors - penetration, joint region width and crack appearance. It was clear from the magnification images, that several geometries appeared in better condition than in the traditional surface geometry, as no cracks is visible in the welded joints. In traditional type A, micro-cracks are visible and appeared in the magnification images. While, in Serie 1, B and D no cracks appeared, but minute cracks are visible in specimen C. In Serie 2-E, F and G, no cracks are presented in all magnification images. In the combination, Serie 3-H and I types, there are no minute cracks and these geometries are better than traditional type A. For Serie 4-J and K, all magnification images showed no cracks. Finally, in the combination in the Serie 5-L and M, minute cracks were visible in the magnification images.

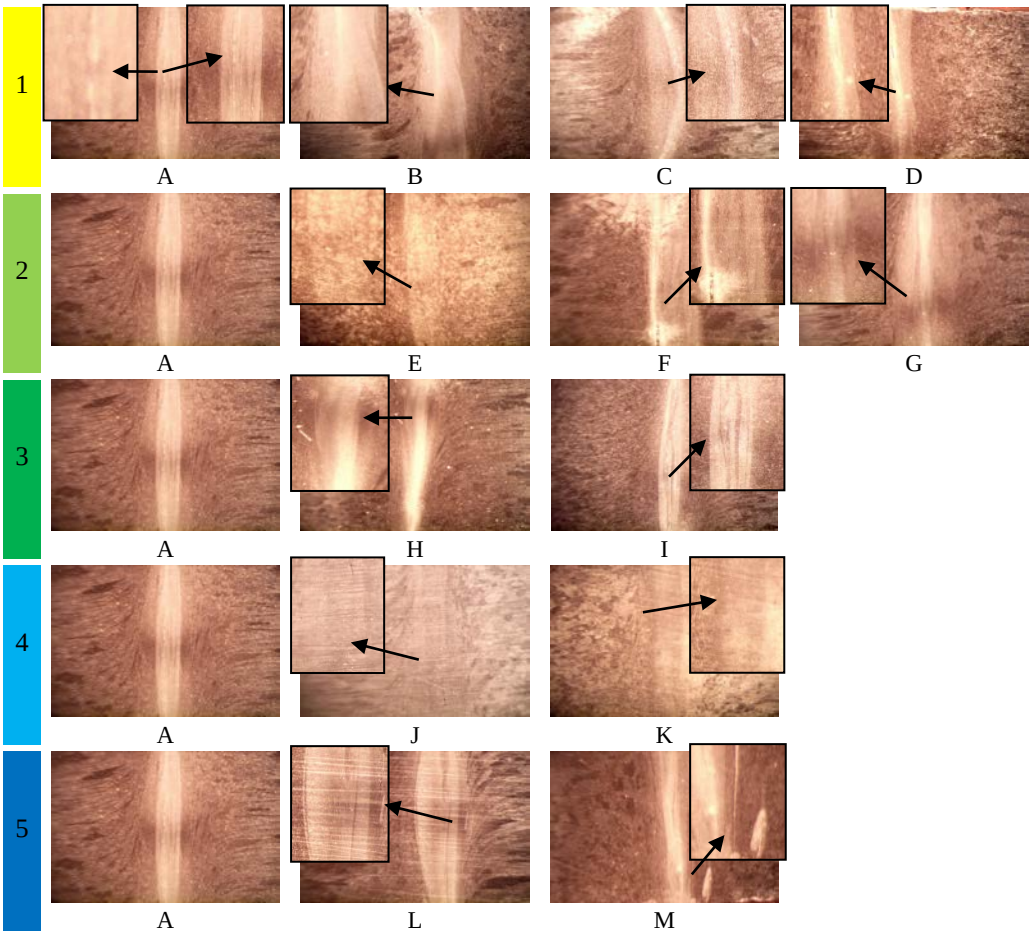

Fig. 9. Microscopic photographs of all specimens, five series

4.2. Hardness profile: Hardness profiles were determined parallel to the bond center line (line II) as well as across the bond lines I and III as schematically shown in Fig. 8. The figures 10 to 14 illustrate the hardness profiles of the similar joints produced with the parameters shown in Table 2.

As seen from the figures the microhardness values of the Aluminum alloy within the line II “bond region” are not constant. This means that there is no regular deformation in the radial direction. The average value of the microhardness is 94 HB. The microhardness of the traditional type A, the base material is slightly higher having an average microhardness value of 100 HB. The radial microhardness of the type A alloy was nearly constant in the range from 95 to 100 mm and then dropped to a minimum at the rotation center. The maximum average microhardness is 100 HB in the line I and 95 HB in the line II. The range of minimum microhardness corresponds to the width of the unaffected area of type A, adjacent to the bond line, as shown in Figure 8. At the position of ±15 mm from the bond line, the radial microhardness is increasing up to a maximum of 100 HB. The difference in values between the base material and the unaffected area at the rotating center of type A is due to strain hardening. The response of type A to the applied friction welding parameters is essentially more pronounced than the type B.

The main issue in IFW is that the material is affected by the friction, which means that “rising temperature” will anneal and lose the rotary centre. Thus, the metal will move away from the rotary centre line in "centrifugal movement". Due to the high rotary movement which causes high cooling state "at the outside surface", the flash part material will solidify hindering continuous pressure for maintaining the integration between the two parts "high force required although increasing the temperature at the rotary centre line".

The hardness evaluation is considered at the centerline (zone) "welding region (-5-5) mm" of the traditional surface profile.

Serie 1: (Fig. 10-A) shows differences in the values. The differences refer to the translation difference of the welding region during the process toward the circumferences. Two types of cooling conditions are involve, fast cooling at the circumferences, due to direct contact with the air, and low rate of the cooling at the center region, due to keeping contact at the center metal.

Keeping those differences at the Serie 1, but with different levels, (Fig. 10-B, C, D), a clear improvement is observed when increasing the radius of the profile from (7.5-15 mm), as well as when increasing the hardness at the centerline more than at the outer regions. The values are kept between 91-100 HB:

- All the evaluations are compared to type A (Fig. 10-A).
- Less effect on the base metal is maintained at type B (Fig. 10-B).

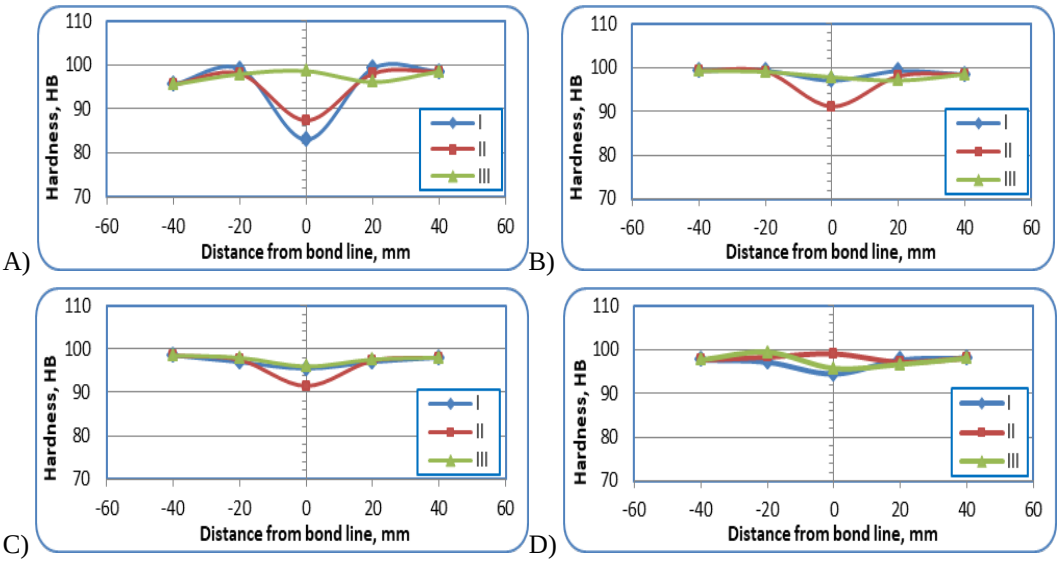

Fig. 10. Microhardness values of the series 1: A, B, C and D

Serie 2: shows the following (Fig. 11):

- Hardness decreases at type E, due to weak bonding at the circumference, while high value are recorded at the center (Fig. 11-E).
- Hardness increases at the centerline region slightly for all types.
- Similar behavior of the values are recorded at types F and G (Fig. 11-F and G).
- Hardness levels are maintained at the stationary part, compared with the rotation part, which dropped 2% at 20 mm distance from the centerline.

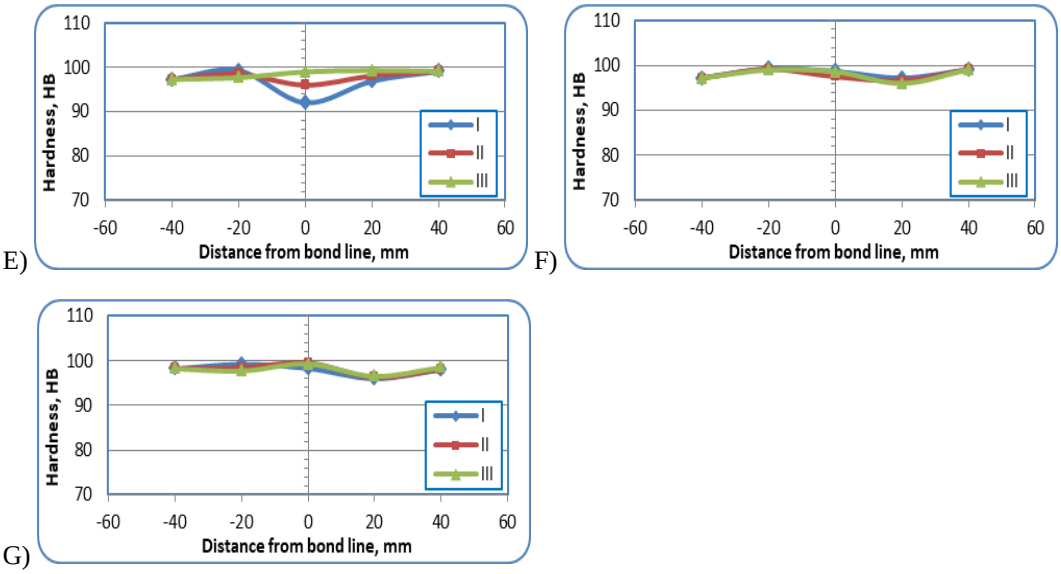

Fig. 11. Microhardness values of the series 2: E, F, and G

Serie 3: shows the following (Fig. 12):
- Hardness changes are concentrated in the center region between -5 to 5 mm (Fig. 12-H and I).
- Hardness distributions of the surface profile are optimized for type H (Fig. 12-H).
- Hardness of all levels deccrease at the welding section, Fig. 12-I (circumference and at the center zone).

H) 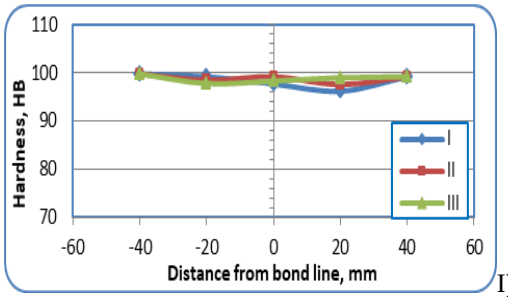

I) 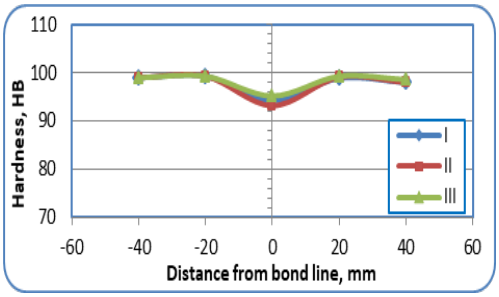

Fig. 12. Microhardness values of the series 3: H and I

Serie 4: shows the following (Fig. 13):
- Hardness charging values are concentrated in the welding region.
- Hardness values decrease at the centerline for both profiles (J and K) (Fig. 13-J and K).
- Clear changes occur in this series.
- Pre-surface contact profile effects appear on the region (B) inversely between J and K profile type.
- Even in the circular section of the part, different hardness values appear at the circumference.
- Hardness values increase at the centerline 1.6 %, from J to K profile.
- No obvious effect on the base metal of the stationary part.

J) 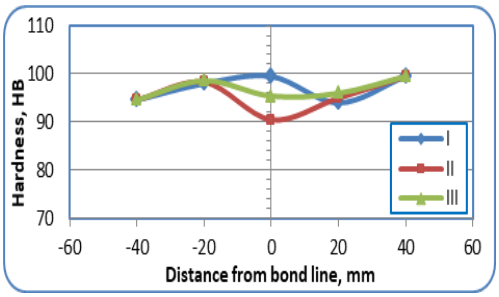

K) 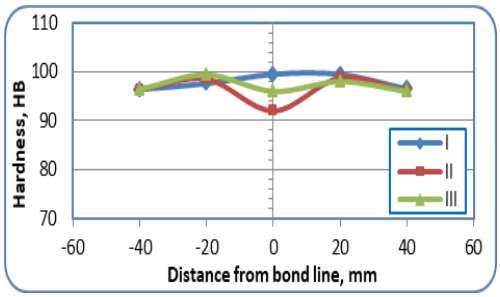

Fig. 13. Microhardness values of the series 4: J and K

Serie 5: shows the following (Fig. 14):
I. In the traditional IFW “type A”, the flash is oriented toward the outside circumferences, affected by centrifugal movement. The internal ring projections

as presented in the types L and M (Fig. 14-L and M), causing to divert the flash metal toward inside as well. The internal ring projections are divided into two parts: toward the outside circumferences (removed by machining); and toward the inner region (observed in the welding interface).
Resulting from that, the hardness values decrease totally at the welding region, as well at the circumferences, being lower than at the centerline by 23.4% (98 HB base metal, 86 HB center line, 75 HB circumferences).
II. the selective projections are working as "not sharp" milling tooltips. The behavior of the flash movement is toward the outside joint interface with the pulses. A small amount of the flash metal moves to fill the spaces between the projections. The following were observed:
- Hardness value decreases to 81 HB at the center line, by 17.3 % comparing to the base metal.
- Region B of the rotation part is affected, decreasing the hardness value to 90 HB "highest reduction comparing to the other profiles".

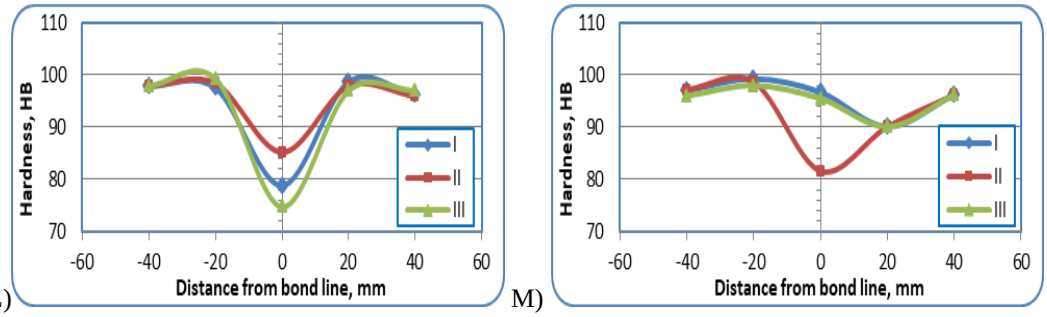

Fig. 14. Microhardness values of the series 5: L and M

As explanation of the series 1 to 4, the amount of the flash material is not completely removed from the welding region. The primary profile design of the Serie 5 involves internal and external flash and depending on the material amount involved in the profile, the amount of the flash material appears around the circumference of the welding circle.

The series 1, 2, 3 and 4 show rising of the microhardness rates at the welding centerlines. The measured values of the microhardness do not exceed the value of the base metal. The series 5 includes the spaces and projections, which caused late friction contact, weak integration and uncomplete bonding.

The best microhardness was measured for type H, (Fig. 12). Slight increasing in HB values of the welded products at the region between (-40 to 0 mm) is recorded.

High drop is measured (less than that of the base metal) in MRH values of the welded products L and M, (Fig. 14).

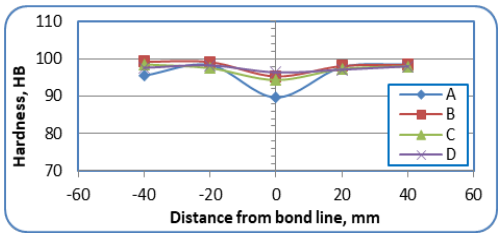

I. Microhardness values of the series 1

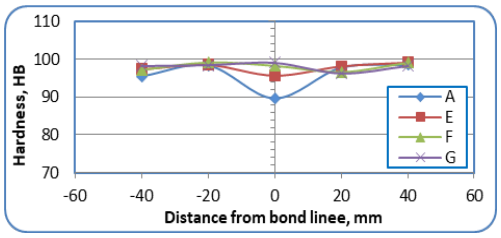

II. Microhardness values of the series 2

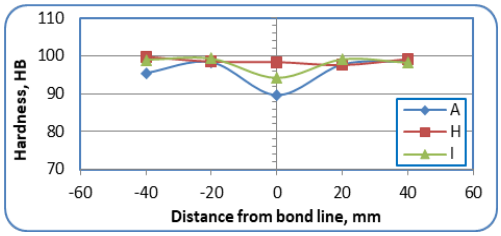

III. Microhardness values of the series 3

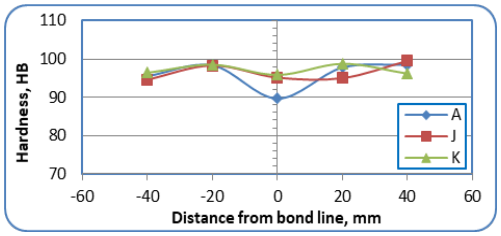

IV. Microhardness values of the series 4

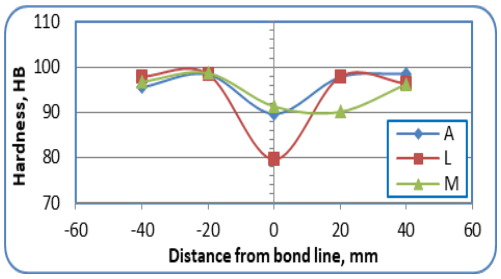

V. Microhardness values of the series 5

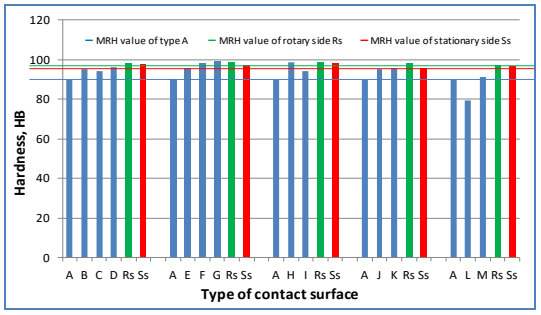

VI. Microhardness average values of the all series hardness average value at the Stationary side, Ss, hardness average value at the Rotary side, Rs

Fig. 15. Microhardness average of the internal structures, Serie 1-5

4.3. Comparing evaluation: The evaluation of the hardness value averages of the series 1–5 is compared with the average values of the base metal hardness (rotary and stationary sides). The summary of the comparing evaluation is presented in Fig. 15-VI:

• high value of type H- Serie 3\ higher value than hardness average values of the base metal;

• low value of type L- Serie 5\ lower value than hardness average values of the base metal;

• the best series are Serie 2 and Serie 4\ higher values than the hardness average value of the base metal (rotary and stationary sides);

• increment average values with increase in the contact surface area of series 2;

• irregular hardness average values of Serie 1, although regularly increasing of the contact radius;

• less effect of hardness average values of type J and K– Serie 4, when compared with each other;

• hardness average values that are measured of all types are higher than type A (traditional type), accept type L – Serie 5.

5. Conclusions

- The change in the pre-surface causes modifications the contact area, which is determined by the change in the friction effect and melting time.
- Increasing the heat rate in the friction welding depending on several variables was observed, including the contact area, and this variable involves the contact profile area per distance during the process.
- The pre-surface of the welded parts is affecting the flash material distribution, inner and outer joint interface. Referring to that, the amount and the place of the flash material have influence on the microhardness values and on the microstructure "profile of the joint and appear or disappear the cracks".
- Preparing the pre-surface of the friction weld parts, while maintaining a part of flash material inside the welded joint gives better hardness properties than the traditional friction welding type, the best profile was type H.
- The variation in the pre-surface caused change in the pressure upset and the flash distribution, therefore the microhardness values were modified along the joint region in depth and in the axial direction (type L and M).
- The levels of microhardness values are different depending on the level of the measurement in welded part depth.

R E F E R E N C E S

[1]. *K. Serop*, Manufacturing processes for engineering materials, Addison-Wesley, 1984.
[2]. *** http://www.ifweld.com/about/process/inertia.php.
[3]. *Doyle, Lawrence E.*, Manufacturing processes and materials for engineers, Second Edition, 1969.
[4]. *B. H. Amstead Phillip, F. Ostwald Myron, L. Begeman*, Manufacturing processes, S1 Version, 1987.
[5]. *P. Sathiya, S. Aravindan and A. Noorul Haq,* "Friction Welding of Austenitic Stainless Steel and Optimization of Weld Quality", International Symposium of Research Students on Materials Science and Engineering December, 2004, Chennai, India, pp. 20-22.
[6]. *M. Maalekian, H. Cerjak*, "Modelling the Orbital Friction Welding of Pearlitic Steel Bars", Trends in Welding Research, Proceedings of the 8th International Conference, 2009, pp. 736-741.
[7]. *S. Biljana, S. M.Čačak and R. C. Čačak*, "Physical Model of the Friction Welded Joint of Different Types of Steel", College of Technical Vocational Studies, FME Transactions, **vol. 36**, No 2, 2008, pp.93-97.
[8]. *A. Kurt, I. Uygur, and U. Paylasan*, "Effect of Friction Welding Parameters on Mechanical and Microstructural Properties of Dissimilar AISI 1010-ASTM B22 Joints", Welding Journal, **vol. 90**, 2011, pp. 102-106.
[9]. *V. Ventzke, H. G. Brokmeier, P. Merhof and M. Koçak*, "Microstructural characterization of friction welded TiAl-Ti6Al4V hybrid joints", Solid State Phenomena, **vol. 160**, 2010, pp. 319-326.
[10]. *K. Mieczyslaw and W. Radoslaw*, "The microstructure and mass transport during friction welding of ductile cast iron", Industrial Lubrication and Tribology **vol. 65**, no. 4, 2013, pp. 251-258.
[11]. *L. Fu, L. Y. Duan, and S. G. Du*, "Numerical Simulation of Inertia Friction Welding Process by Finite Element Method", Northwestern Polytechnical University, Xi'an, China. Welding journal, 2003, pp. 65-70.
[12]. *S. A. A. Akbari Mousavi and A. Rahbar Kelishami*, "Experimental and Numerical Analysis of the Friction Welding Process for the 4340 Steel and Mild Steel Combinations", Welding Journal, **vol**. 87, 2008, pp. 178-186.